CHAPTER 4

Design and Optimization of Genetically Encoded Fluorescent Biosensors: GTPase Biosensors

Louis Hodgson,[*] Olivier Pertz,[†] and Klaus M. Hahn[*]

[*]Department of Pharmacology
Lineberger Cancer Center
University of North Carolina at Chapel Hill
Chapel Hill, North Carolina 27599

[†]Institute of Biochemistry and Genetics
Department of Clinical-Biological Sciences (DKBW)
University of Basel, Center for Biomedicine,
CH- 4058 Basel, Switzerland

METHODS IN CELL BIOLOGY, VOL. 85

0091-679X/08 $35.00
DOI: 10.1016/S0091-679X(08)85004-2

Abstract

This chapter details the design and optimization of biosensors based on a design used successfully to study nucleotide loading of small GTPase proteins in living cells. This design can be generalized to study many other protein activities, using a single, genetically encoded chain incorporating the protein to be studied, an "affinity reagent" which binds only to the activated form of the targeted protein, and mutants of the green fluorescent protein (GFP) that undergo fluorescence resonance energy transfer (FRET). Specific topics include procedures and caveats in the design and cloning of single-chain FRET sensors, *in vitro* and *in vivo* validation, expression in living cell systems for biological studies, and some general considerations in quantitative fluorescence imaging.

I. Introduction

Direct visualization of proteins in their native environment has been a powerful tool in cell biological studies for over two decades (Taylor and Wang, 1980). Early approaches were limited in scope to proteins that could be purified *in vitro*, chemically labeled, and reintroduced into cells via methods such as microinjection and electroporation. The applicability of biosensors was greatly expanded by the discovery of the green fluorescent protein (GFP) from the jellyfish *Aequorea victoria* (Chalfie *et al*., 1994; Heim and Tsien, 1996) and very importantly by the development of mutants with enhanced photophysical properties and the ability to undergo fluorescence resonance energy transfer (FRET). Nonradiative FRET between different spectral variants of fluorescent proteins is strongly dependent on the distance and orientation between the GFP mutants. This property can be used to design genetically encoded biosensors that report posttranslational modifications and conformational changes, rather than simply tagging proteins to follow changes in protein localization. There are now multiple proven biosensors based on FRET between GFP mutants (Adams *et al*., 1991; Hahn *et al*., 1992; Haj *et al*., 2002; Llopis *et al*., 2000; Miyawaki *et al*., 1997; Ting *et al*., 2001). Figure 1 illustrates several of these biosensors, including the RhoA activation sensor from our laboratory that is used as an example in this chapter.

FRET signals are often weak relative to fluorescence background, easily leading to false interpretations, or alternately requiring biosensor expression levels that perturb normal cell physiology. Here, we will examine how to optimize biosensor design characteristics that impact fluorescence properties, and discuss controls that validate the biological information obtained from living cells. We will attempt to lay out a straightforward procedure to develop biosensors, based on our experience with the p21 Rho family of small GTPases. Fluorescence microscopy will not be covered in detail in this chapter; readers are referred to previous publications in this area (Gordon *et al*., 1998; Hodgson *et al*., 2006; Kenworthy, 2001; Periasamy, 2001; Periasamy and Day, 1999; Xia and Liu, 2001).

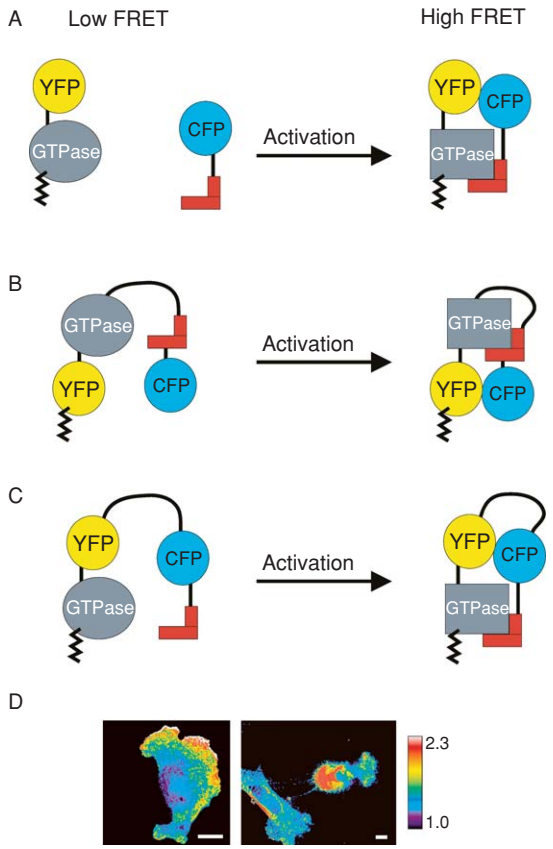

Fig. 1 Examples of biosensors based on fluorescence resonance energy transfer (FRET) between the green fluorescent protein (GFP) mutants. (A) Intermolecular FRET. The donor and the acceptor fluorophores are attached to two separate molecules, the targeted protein and an "affinity reagent" that interacts only with the activated state of the target. Activation of the target causes the two to bind, generating FRET. (B) Intramolecular FRET. Fluorescent proteins are placed on the N- and C-termini, so that the separation between the fluorophores is strongly dependent on protein activation. Activation results in the interaction of the affinity reagent with the target protein, leading to increased FRET. In some cases, the C-terminal end of the biosensor is modified to attach a lipid modification motif from K-Ras, producing constitutive membrane localization. In other cases, proteins are placed in the internal portion of the biosensor. This design is advantageous when the C-terminus of the protein must remain intact for the normal regulation of subcellular localization. (C) Images of the RhoA biosensor in living mouse embryonic fibroblasts during motility. Ratiometric images in pseudo-color show RhoA activation during tail retraction (right) and in extending protrusions at the cell's leading edge (left). Scale bar, 20 μm. Images reproduced from Pertz *et al.* (2006).

II. Background: Factors Influencing FRET Efficiency

FRET is sensitive to both the distance and orientation of the two fluorophores in the biosensor—when the fluorophores are sufficiently far apart or have orthogonal dipole orientations, excitation of the donor simply leads to donor emission rather than to FRET. However, when the distance is sufficiently small, and the orientation enables sufficient dipole coupling, excitation energy is transferred from the donor to the acceptor, leading to decreased donor emission and increased emission from the acceptor. This produces a characteristic FRET excitation/emission spectrum, different from that of the donor or the acceptor alone.

There has been a continuing evolution of useful GFP mutants suitable for FRET in living cells. Mutants incorporate different trade-offs between brightness, FRET efficiency, photostability, and the pH dependence of fluorescence characteristics (Heikal *et al.*, 2000; Miyawaki and Tsien, 2000). Enhanced brightness improves the overall signal-to-noise ratio in cells, but is not always an improvement if it comes at the cost of FRET efficiency (which affects the difference between the activated and inactivated states of the biosensor) (Nguyen and Daugherty, 2005). The cyan and yellow fluorescent proteins (CFP and YFP) (Miyawaki and Tsien, 2000) are relatively fast maturing, bright GFP mutants that have proven useful in many FRET biosensors. More recent mutants with improved FRET efficiency (Nguyen and Daugherty, 2005) include CyPet and YPet, which exhibit 6.7-fold greater FRET efficiency than the original CFP–YFP pair does (Nguyen and Daugherty, 2005). In this chapter, we will refer to the GFP mutants simply as CFP and YFP.

FRET efficiency is quantified by the Förster equation:

$$R_0 = [8.8 \times 10^{23} K^2 n^{-4} Q_d J]^{1/6}$$

R_0 is the Förster distance, where energy transfer is 50% efficient. K^2 is the dipole orientation factor, a function of the donor emission transition moment and the acceptor absorption transition moment. $K^2 = 2/3$ is generally assumed when fluorophore rotation can occur about the bond attaching the fluorophore to the protein. Q_d is the fluorescence quantum yield of the donor in the absence of the acceptor, n is the refractive index of the medium, generally assumed to be 1.4 for proteins, and J is the spectral overlap integral, indicating the extent of overlap between the donor fluorescence emission spectrum and the acceptor excitation spectrum (Lakowicz, 1999).

In biosensors, the activation of the targeted protein affects FRET efficiency by altering the distance and/or the orientation of the fluorophores. FRET efficiency, E, is exquisitely sensitive to the distance between the fluorophores:

$$E = \frac{R_0^6}{(R_0^6 + R^6)}$$

In this equation, R_0 is the Förster distance and R is the actual distance (Lakowicz, 1999). FRET varies as the power of 6 of the distance between the fluorophores. R_0 is dependent on the dipole orientation factor K^2. The K^2 factor can be assumed to be 2/3 only when both fluorophores are free to rotate isotropically during the excited state lifetime. A change in the rotational mobility or fixed angle of the fluorophores in different biosensor states can also affect FRET (K^2 can change between 0 and 4) (dos Remedios and Moens, 1995; Lakowicz, 1999). The effects of fluorophore separation (linear displacement) versus angular reorientation cannot be readily separated in live cell studies. Therefore, FRET changes are not used to precisely determine distances between proteins. Rather, the extent of FRET produced by fully activated versus inactive target protein is determined, and these endpoints are used to interpret FRET signals in cells.

III. Design and Cloning of Biosensors

In single-chain FRET biosensors, the target protein is linked to the affinity reagent and to two fluorescent proteins (Fig. 1). This can affect the interactions of the target protein with upstream regulatory proteins, downstream effectors, and scaffolding proteins. Preservation of upstream regulatory interactions is most important, as these affect the activation being monitored. Competing with effector interactions need not invalidate biosensor readouts, provided these interactions do not impact biosensor localization, and provided the biosensor can be expressed at low concentrations that minimize dominant negative effects. In fact, effects of biosensor overexpression can be reduced when the affinity reagent competes with native effectors. Pull down experiments demonstrated that the affinity reagent in the RhoA biosensor competed effectively against native effectors (Pertz *et al*., 2006).

Validation of biosensors must include experiments to determine if the reported protein localization has been perturbed by the modification of the target protein, to determine which ligands are being affected, and to determine intracellular biosensor concentrations below which normal cell function is not affected. Point mutations in the biosensor that block interaction between the affinity reagent and the target protein should knock out activation signals, while activating mutations should lead to maximal activation. The effects of such mutations on pull down of endogenous ligands can reveal how the target protein's interaction with various ligands is affected by competition with the affinity reagent in the biosensor. The ability to pull down competing ligands should be increased when point mutations knock out the affinity reagent interactions (see Pertz *et al*., 2006, supplementary data). The distribution of the fluorescent biosensor should mimic that of the native protein visualized via antibody staining, or at least the GFP fusions of the target protein. Finally, the biosensor should not perturb normal cell behaviors known to be mediated by the target protein. Usually, this is a function of

intracellular biosensor concentration. Although precise concentrations are very difficult to measure, it is not so challenging to determine a concentration cutoff above which experiments should not be performed. In a population of randomly loaded cells, a plot of brightness/area versus inhibitor effects usually reveals clear cutoffs where biological perturbation occurs (Chamberlain *et al.*, 2000; Kraynov *et al.*, 2000; Nalbant *et al.*, 2004).

The placement of the GFP mutants in the biosensor chain can be varied, to affect which portions of the target protein are exposed to biological interactions. In our RhoA GTPase biosensor, we were forced to alter the usual arrangement of components. Previous biosensors had placed the GFP mutants at the termini of the chain, so that the separation of the GFP mutants would be maximally affected when the affinity reagent changed between the bound and unbound states. However the Rho family GTPases require an intact C-terminus to interact with guanine nucleotide dissociation inhibitors (GDI). GDI control reversible membrane localization of the GTPases (Bokoch *et al.*, 1994; Chuang *et al.*, 1993; DerMardirossian and Bokoch, 2005). Through optimization of linker length, we were able to place the GFP mutants on the interior of the chain, between the target protein and the affinity reagent (Fig. 1). Here changes in the orientation of two GFP mutants may have played a larger role.

To maximize FRET changes, the length of the linker connecting the intrachain fluorescent proteins had to be optimized. We used a flexible linker of 18 amino acids, encoding "GSTSGSGKPGSGEGSTKG" (Whitlow *et al.*, 1993) in tandem cassettes. The linker encoded a *Bam*HI restriction site on the 5′ side and *Bgl*II site on the 3′ side. These two restriction sites form compatible termini when cut, but ligated product cannot be cut by either of the enzymes. The sense and antisense oligonucleotides were produced with 5′-phosphorylation modification (Invitrogen) and were annealed and ligated for 1 h using T4 DNA ligase in the presence of *Bam*HI and *Bgl*II enzymes. This produced a ladder of multiple linker lengths containing different cassette units. We cloned this mixture into the biosensor backbone to obtain 1–4 linker cassette versions whose FRET efficiency was compared.

The choice of the affinity reagent is one of the most important factors determining the sensitivity of the biosensor. Ideally, there should be a large difference in affinity for the active versus inactive target protein. Low-affinity binding is greatly increased when the affinity reagent is incorporated in the same chain as the target protein. This can reduce the FRET change between the bound and unbound states, because the affinity reagent shows substantial binding even to inactive target. In such cases, the biosensor produces an elevated FRET:CFP ratio even when dominant negative GTPase mutants are used. We have found that subtle differences in affinity can strongly impact the functioning of the biosensor.

In order to facilitate the optimization and the cloning of various GTPases and binding domains, we developed a "master construct" based on the pTriEX-4 backbone (EMD Chemicals Inc, San Diego) that contains multiple, unique restriction sites between every component of the single-chain biosensor (Fig. 2; sequence

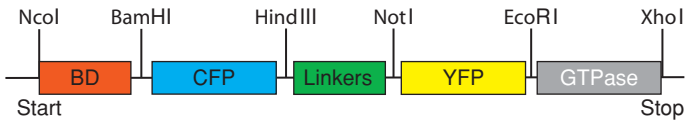

Fig. 2 Schematic representation of the biosensor DNA construct in pTriEX4 vector. The indicated restriction sites are unique sites. (See Plate no. 10 in the Color Plate Section.)

information in Appendix I). We used this construct to develop and optimize several GTPase biosensors including the published RhoA biosensor (Pertz *et al.*, 2006).

IV. Validation of the Biosensor in Cell Suspensions

The single-chain biosensors are quite large (>90 kDa) and so cannot readily be expressed and isolated for *in vitro* characterization (i.e., of FRET, target response, and effect of ligands). However, they can be characterized by expressing biosensors in cells suspended in a fluorometer cuvette. We use HEK293T cells because of their transfection efficiency: expression levels must be high to detect the biosensor changes in cell suspension. When we test response by coexpressing ligands, coexpression must occur in a large percentage of cells. The constitutively active and dominant negative mutants of the biosensor are compared, and the sensitivity to ligands that affect activation is examined by coexpressing the biosensor and the ligand [litration of DNA concentrations is critically important. Typically one- to fourfold excess of regulators, for RhoA including GDI, GEF, and GTPase activating protein (GAP)]. Adherent cells are transfected, then detached and measured as a suspension in the fluorormeter cuvette without lysis. Lysis in some cases releases factors that strongly affect the activation of the target protein, overwhelming the overexpressed regulatory protein.

Despite variable transfection efficiency and cell health, we have found that this assay provides robust and repeatable readouts of the biosensor behavior. Importantly, the overexpression of GTPases in HEK293T cells saturates endogenous cellular regulators, so that the overexpressed biosensor containing wild-type target protein will be "all-on" and will give a signal like that of the overexpressed constitutively active mutants. For RhoA, the overexpressed wild-type protein overwhelms the capacity of native GDI to maintain the biosensor in an inactive state. Usually, a fourfold excess cotransfection of GDI results in an "all-off" readout, similar to that of the dominant negative biosensor, biosensor that cannot bind the affinity reagent, or the coexpression of GAP.

Biosensors can efficiently be developed through a series of optimization steps. The optimization of the linker length is best carried out first, using relatively straightforward tests of biosensor response (i.e., for GTPases, the effect of GDI coexpression, as described above). The procedure described above can be used to test linkers between 1 and 4 of repeating units. Depending on the trend of the

response, it may be necessary to further shorten the linker to GSGSGS or lengthen to 5–6 linkers. The biosensors with the best response and brightness are further validated using point mutations and more complex tests of interaction with regulatory ligands (i.e., biosensors containing the activated and inactivated GTPases, and effects of GEFs and GAPs) (Pertz *et al.*, 2006). Finally, the best biosensor is introduced into viral transduction vectors (see Section IV.B).

In many cases, cells are very sensitive to biosensor expression levels; viral transfection of inducible vectors, and stable cell lines with low-expression levels must be used. This is often important not only to avoid toxicity but also because biosensor response is seen only at lower expression levels. As described above, our RhoA sensor is constitutively "on" when overexpressed, because it overwhelms endogenous GDI. An uncautious experimentalist using higher levels of sensor to overcome typically weak FRET fluorescence might simply assume that the sensor did not work.

It may be possible to alter the relative orientations of the components to effect the changes in the FRET efficiency using circularly permutated fluorescent proteins (Baird *et al.*, 1999; Nagai *et al.*, 2004). We have implemented this to greatly enhance the FRET ratio changes of some biosensors (approximately threefold increase in ratio change, unpublished data). With circularly permutated fluorescent protein built into the biosensor, the intrachain linker lengths need to be reoptimized.

The following sections describe more detailed procedures for some of the steps outlined above.

A. Expression in HEK293T Cells for Assay of Biosensors in Cell Suspension

This is a protocol for testing the effects of protein coexpression on the RhoA biosensor. It can provide a template for the development of other GTPase biosensors.

1. *Day 1, 3 days before the assay*: Prepare 6-well plates by coating the wells with a 1:10 dilution of polylysine (P4832–50 ML; Sigma Co, St. Louis, MO) in 1 ml PBS per well for 1 h at room temperature on a rocker. Prepare enough wells to test each condition in triplicate, plus 1 extra well for mock transfection (this will be used to obtain the background fluorescence on the fluorometer). HEK293T cells should be detached and plated onto polylysine coated 6-well plates at (5–6) $\times$ 10^5 cells per well. This should be optimized in the given range, depending on cell health and the doubling rate.

2. *Day 2*: On the following day, transfect typically 500–750 ng DNA per well, using the following ratios and the Lipofectamine Plus (Invitrogen, Carlsbad, CA) protocol:

   a. Biosensor and GDI: 100 ng biosensor DNA and 400 ng GDI DNA. In those wells containing only biosensor DNA (GDI negative), make sure to equalize the total DNA quantity by cotransfecting control empty vector.

b. Biosensor mutants: 100 ng wild-type biosensor plus 400 ng empty vector, and 100 ng biosensor mutants plus 400 ng empty vector. Also prepare biosensor plus GDI (100:400 ng) as a control.
c. GEF-rescue of GDI binding: 100 ng biosensor DNA, 400 ng GDI DNA, and 100 ng GEF. Variable amounts of GEFs have been needed to rescue the GDI binding, depending on the relative efficiency of the GEF DH-PH expression constructs. In some cases such as Dbl, Dbs, and Intersectin, we have had to use 100 ng to see effects without affecting cell viability. Other GEFs, including Tiam-1, can be used at higher concentrations. We have used ratios form 1:4:1 to 1:4:10, depending on the particular GEF/biosensor combination.
d. GAP inhibition of biosensor: 100 ng biosensor DNA and 100–400 ng GAP DNA. Here, excess GAP will be toxic and each GAP DNA should be titrated.

Suspend the DNA into 100 μl of serum and antibiotic-free DMEM. Add 16 μl of Plus reagent (Invitrogen). Vortex and let stand for 15 min at room temperature. Add to this mixture 100 μl of serum and antibiotic-free DMEM containing 5 μl of Lipofectamine reagent (Invitrogen). Vortex and let stand for 15 min at room temperature. While the transfection mixtures are incubating, wash the cells on 6-well plates once with PBS and add 0.8 ml of serum and antibiotic-free DMEM into each well. Apply the transfection mixture into the wells, swirl to mix fully, and incubate under standard tissue culture conditions for 6 h. At the end of this incubation, exchange medium with standard culture medium, adding 3 ml of medium per well.

3. *Day 3*: Check fluorescence—it is particularly important to check for proper localization of the biosensor, especially if GDI and GEFs are coexpressed. There should be distinct membrane or cytosol localization, depending on the conditions used (Pertz *et al*., 2006). For this purpose, a tissue culture microscope equipped with FITC/GFP epifluorescence filters should suffice.

4. *Day 4*: On the day of the assay, cells are washed once with PBS, and 1 ml per well of trypsin/EDTA is added and immediately aspirated. Using 0.5 ml of chilled PBS, cells are detached by repeated pipetting and placed on ice. The samples are then read on the flourometer by placing 0.4 ml of the cell suspension into the fluorometer cuvette (18/9F-Q-10; Starna Cells, Inc., Atascadero, CA). Fluorescence emission scans are performed by excitation at 433 nm and scanning between 450 and 600 nm, stepping every 3 nm. Mock-transfected (empty vector control) cells should be used to obtain the background spectra, which should be subtracted from all subsequent measurements. The spectra should be normalized to the maximum CFP emission at 477 nm to standardize the data analysis. The ratio of FRET emission at 525 nm to the CFP emission at 477 nm is compared among various mutants and transfection conditions.

In Fig. 3, sample validation results for the single-chain RhoA GTPase biosensor are shown.

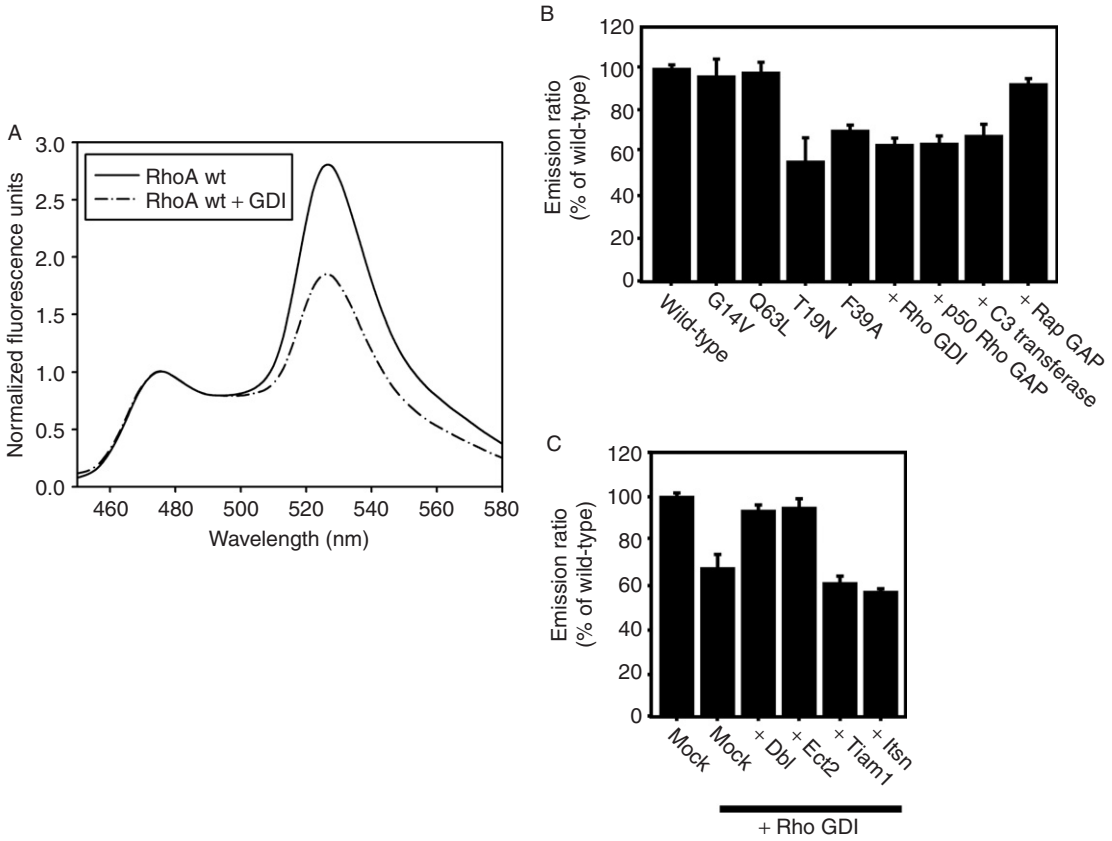

Fig. 3 *In vitro* validation of the single-chain cyan and yellow fluorescent proteins fluorescence resonance energy transfer (CFP–YFP FRET) RhoA biosensor. (A) Emission spectra for the wild-type RhoA biosensor alone and the biosensor plus guanine nucleotide dissociation inhibitors (GDI) coexpression. (B) Versions of the biosensor incorporating the indicated mutations in the GTPase. GDI coexpression shows interaction with G14V constitutively active mutant, but not with Q63L constitutively active mutant. (C) The reduced ratio produced by the expression of excess GDI is rescued by the coexpression of the GEFs Dbs or Dbl, but not by Intersectin (a Cdc42 GEF) or Tiam-1 (a Rac GEF). p50RhoGAP expression results in a low ratio. Data panels reproduced from Pertz *et al.* (2006).

B. Expression of the Biosensor in Cells

The pTriEX backbone used for the cloning of biosensors allows overexpression in mammalian cells driven by the *Cytomegalovirus* (CMV) promoter. However, this expression strategy requires that one is aware of the potential toxicity of GTPases upon overexpression (Pertz *et al.*, 2006) and the need for a near-stoichiometric relationship between endogenous GTPases and endogenous regulators in cells (Del Pozo *et al.*, 2002; Michaelson *et al.*, 2001).

We have addressed these issues by using retroviral transduction to stably incorporate low copy numbers of the biosensor DNA (Pertz *et al*., 2006). Transfected cells were sorted by fluorescence activated cell sorting (FACS) to obtain low expressors only, so that the biosensor expression level was comparable to endogenous GTPase. We have shown that the competition with endogenous effectors of the GTPase is not a significant problem (Pertz *et al*., 2006).

In order to address the toxicity of the biosensor expression, we used a tetracycline-inducible retroviral construct based on a pBabe-Sin-Puro-tet-CMV backbone. We use the tet-off stable MEF/3T3 cell system (Clontech Mountain View, CA), and the infected cells are repressed using 1 μg/ml Doxycyclin. Cells are selected with Puromycin up to 10 μg/ml, increased gradually in concentration following the infection. At the end of the selection, cells are induced for the biosensor expression by the removal of Doxycyclin and reseeding at a sparse concentration (1×10^4 cells per 10 cm TC dish) for 48 h. These cells are then sorted by FACS to produce near 100% cells positive for the biosensor expression, which are then repressed again with the application of Doxycyclin.

For experiments, it is important to use sparse reseeding following the removal of Doxycyclin from the culture media. We routinely maintain repressed cells in 1 μg/ml Doxycyclin in standard tissue culture conditions. For induction, cells are detached by a brief trypsinization and spun at 1200 rpm for 5 min. Supernatant media are suctioned out carefully and completely, and cells are resuspended in fresh culture medium without Doxycyclin. Cells are replated at 1×10^4 cells per 10 cm TC dish without Doxycyclin and checked for fluorescence 24 h after the induction. The cells are kept in this condition for an additional 24 h before the assay. This additional 24 h will ensure that overexpressors will die off, and cells only with a sustainable expression level will survive for the experiment. Cells are detached and replated on coverslips coated with fibronectin (10 μg/ml; Sigma) on the morning of the experiment and allowed to adhere for 5 h before imaging.

V. Microscopy and Imaging Considerations

The basic aspects of the fluorescence imaging using FRET biosensors have been covered elsewhere (Gordon *et al*., 1998; Kenworthy, 2001; Periasamy, 2001; Periasamy and Day, 1999; Xia and Liu, 2001). It is worthwhile to mention a few key points that apply specifically to the use of the single-chain biosensors at low-intracellular concentrations.

Unlike single-chain FRET biosensors, intermolecular FRET biosensors (Chamberlain *et al*., 2000; Kraynov *et al*., 2000; Tzima *et al*., 2003) require bleed-through corrections due to the varying subcellular distribution of the two components. They do produce enhanced dynamic range. For a single-chain design, it is sufficient to simply take a ratio of the FRET emission over the donor emission

(Pertz *et al.*, 2006). For both designs, it is important to realize that the two fluorophores will bleach at different rates, so that the bleaching corrections are required to counter a bias in the signal over time. The computational steps involved in the calculation of ratios and photobleach correction are covered elsewhere (Hodgson *et al.*, 2006).

For the relatively dim fluorescence we use to maintain biosensor concentrations that do not overwhelm endogenous regulatory molecules, we must be careful to maximize the efficiency of light collection. It is not desirable to compensate for low biosensor concentrations simply by increasing irradiation, as this bleaches the biosensor and increases the phototoxicity. We routinely use an oil immersion 40× DIC (differential interference contrast) objective with a numerical aperture of 1.3, together with 2 × 2 binning on our charge coupled device (CCD) camera. Using 60× or higher magnification objective lens cuts down greatly on the brightness of the transmitted signal. It is important to use a DIC rather than phase contrast objective lens, as the phase objective contains a phase ring that substantially reduces the transmittance of light through the objective lens. Neutral density filters of 0.6–1.0 (54.9–36.8% transmittance) are used to cut the brightness of the excitation light. Longer exposure using dimmer excitation light is preferable to shorter, more intense irradiation; this reduces both bleaching and phototoxicity. We routinely use methods to remove oxygen from the medium to further decrease photobleaching and phototoxicity [an oxygen scavenger reagent, OxyFluor (Oxyrase, Inc.), antioxidants including vitamin C at 1 mM concentration, and/or purging the assay medium with Argon; Fig. 4].

We currently use a Sony ICX285-based interline transfer cooled CCD camera, the Roper/Photometrics CoolSnapESII, cooled to 0 °C. This camera can be

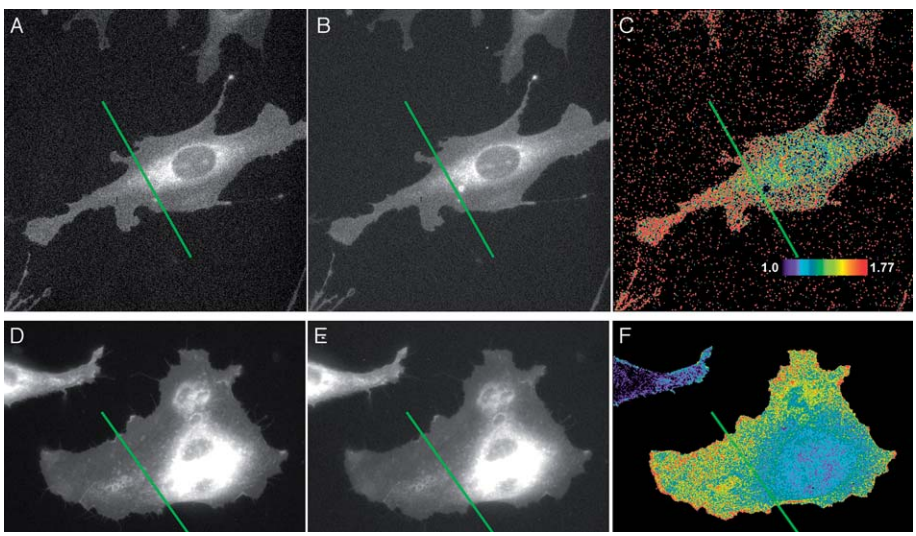

Fig. 4 (*continues*)

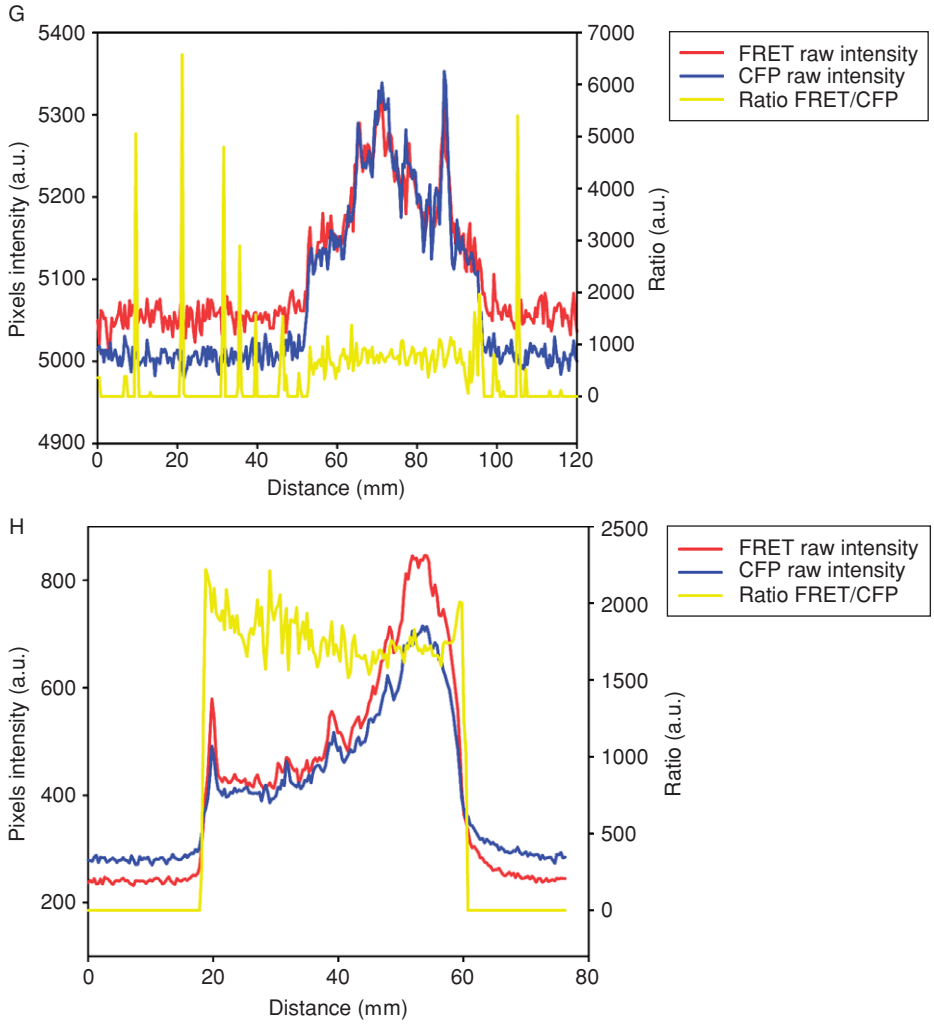

Fig. 4 Comparison between an electron multiplying charge coupled detector (EMCCD) camera and a normal cooled charge coupled detector (CCD) camera for wide-field imaging of a cyan and yellow fluorescent protein fluorescence resonance energy transfer (CFP–YFP FRET) biosensor. (A) FRET and (B) CFP channels taken using a Roper Photometrics Cascade II 512 camera at 1 × 1 binning, 3× gain, 3300 EM-gain, 50 and 100 ms exposures per frame for FRET and CFP, respectively. Both channels were averaged for 10 frames. (C) Ratiometric result (FRET–CFP) from the images shown in A and B. The color bar is scaled from 1.0 to 1.77. (D) FRET and (E) CFP channels taken using a Roper Photometrics CoolsnapES camera at 2 × 2 binning, 2× gain, 400 and 800 ms exposures for FRET and CFP, respectively. (F) Ratiometric result (FRET–CFP) from the images shown in D and E. Scaling is identical to that shown in (C). All images were taken using a Zeiss EC-Plan Neofluor 40× NA = 1.4 oil immersion DIC objective lens, with similar intensities. (G) Line scans from the green lines shown on panels A–C. (H) Line scans from the green lines shown on panels D–F. The raw data from the two cameras (A and B vs C and D) appear similar by visual observation, but the ratio images (C and F) and the line scans reveal higher noise associated with the EMCCD camera. This is due to both the greater stochastic noise in the EMCCD camera raw images and the propagation of this noise when the two noisier images are divided by one another. Thus this issue is more acute where division of image for ratio imaging is required. (See Plate no. 11 in the Color Plate Section.)

obtained with 5 e-read noise, and 0.01e-/pixel/s dark current. The quantum efficiency of the chip is 60% for 450–625 nm light, and it has a small pixel size (6.45 × 6.45 μm) for good spatial resolution. We routinely use 2 × 2 binning and expose 800 ms for CFP and 400 ms for FRET when imaging the RhoA biosensor. These conditions usually result in gray values filling 75% of the full 12-bit range of camera digitization. We do not recommend the current on-chip gain amplification electron multiplying CCD (EMCCD) cameras for biosensor imaging. While these cameras can capture images under extremely dim illumination conditions, the gain-circuitry introduces too much stochastic noise for ratiometric imaging (Fig. 4). The stochastic noise is greatly increased when one image is divided by another. Other viable options may include back-thinned, back-illuminated cooled CCD cameras with high-quantum efficiency. These cameras offer ultra-high quantum efficiency (over 90%), but the pixel size is usually large (16 × 16 μm), reducing spatial resolution.

The choice of imaging medium is also an important consideration when imaging FRET biosensors. Background fluorescence from the media is a significant issue at the wavelengths used. We have performed a quantitative comparison of various media available commercially, and have concluded that Ham's F-12 K medium without phenol red (Kaighn, 1973; Robey and Termine, 1985) is a good choice. Unfortunately, this medium is no longer commercially available. The formulation can be found in Appendix II. Commercially available phenol red-free medium 199 (Mediatech Inc, Herndon, VA) has slightly worse background fluorescence than does Ham's F-12K medium without phenol red.

VI. Conclusion

Here, we present some basic methods for designing, building, and validating single-chain biosensors, with procedures specifically adapted to study small GTPase proteins. The techniques and approaches are potentially applicable to a much wider group of proteins, those where an appropriate binding-domain/target can be identified. We hope that this description of building a single-chain CFP–YFP FRET biosensor, including common pitfalls, will be valuable for those wishing to develop biosensors for their favorite molecule.

VII. Appendix I

A. DNA Sequence for the pTriEX-4-Biosensor Construct

Start (NcoI site) into pTriEX NcoI site, and then 6×His tag plus GSG linker

*CCATGG*CACACCATCACCACCATCACGGTAGTGGC

Rhotekin RBD

ATCCTGGAGGACCTCAATATGCTCTACATCCGGCAGATGGCACT
CAGCCTGGAGGACACAGAGCTGCAGAGGAAACTAGATCATGAG
ATCCGGATGAGGGATGGGGCCTGCAAGCTGCTGGCAGCCTGCT
CCCAGCGAGAGCAGGCTCTGGAAGCCACCAAGAGCCTGCTGGT
GTGCAACAGCCGTATTCTCAGCTACATGGGTGAGCTGCAGCGG
CGAAAGGAGGCCCAGGTGCTGGAGAAGACA

GSG linker (BamHI)

*GGATCC*GGA

CFP (HindIII)

ATGGTGAGCAAGGGCGAGGAGCTGTTCACCGGGGTGGTGCCC
ATCCTGGTCGAGCTGGACGGCGACGTAAACGGCCACAAGTTCA
GCGTGTCCGGCGAGGGCGAGGGCGATGCCACCTACGGCAAGC
TGACCCTGAAGTTCATCTGCACCACCGGCAAGCTGCCCGTGCCC
TGGCCCACCCTCGTGACCACCCTGACCTGGGGCGTGCAGTGCTT
CAGCCGCTACCCCGACCACATGAAGCAGCACGACTTCTTCAAGT
CCGCCATGCCCGAAGGCTACGTCCAGGAGCGCACCATCTTCTTC
AAGGACGACGGCAACTACAAGACCCGCGCCGAGGTGAAGTTCG
AGGGCGACACCCTGGTGAACCGCATCGAGCTGAAGGGCATCGA
CTTCAAGGAGGACGGCAACATCCTGGGGCACAAGCTGGAGTAC
AACTACATCAGCCACAACGTCTATATCACCGCCGACAAGCAGAA
GAACGGCATCAAGGCCAACTTCAAGATCCGCCACAACATCGAG
GACGGCAGCGTGCAGCTCGCCGACCACTACCAGCAGAACACCC
CCATCGGCGACGGCCCCGTGCTGCTGCCCGACAACCACTACCT
GAGCACCCAGTCCGCCCTGAGCAAAGACCCCAACGAGAAGCGC
GATCACATGGTCCTGCTGGAGTTCGTGACCGCCGCCGGGATCA
CTCTCGGCATGGACGAGCTGTACAA*A AGC TT*A

Linker Cassette

ACTTCTGGTTCTGGTAAACCTGGTTCTGGTGAAGGTTCTAC
TAAAGGTGGATCT

Link into YFP (NotI)

GGATCTGCGGCCGCA

YFP (EcoRI)

ATGGTGAGCAAGGGCGAGGAGCTGTTCACCGGGGTGGTGCCC
ATCCTGGTCGAGCTGGACGGCGACGTAAACGGCCACAAGTTCA
GCGTGTCCGGCGAGGGCGAGGGCGATGCCACCTACGGCAAGC
TGACCCTGAAGTTCATCTGCACCACCGGCAAGCTGCCCGTGCCC

TGGCCCACCCTCGTGACCACCTTCGGCTACGGCCTGATGTGCTT
CGCCCGCTACCCCGACCACATGAAGCAGCACGACTTCTTCAAGT
CCGCCATGCCCGAAGGCTACGTCCAGGAGCGCACCATCTTCTTC
AAGGACGACGGCAACTACAAGACCCGCGCCGAGGTGAAGTTCG
AGGGCGACACCCTGGTGAACCGCATCGAGCTGAAGGGCATCGA
CTTCAAGGAGGACGGCAACATCCTGGGGCACAAGCTGGAGTAC
AACTACAACAGCCACAACGTCTATATCATGGCCGACAAGCAGA
AGAACGGCATCAAGGTGAACTTCAAGATCCGCCACAACATCGA
GGACGGCAGCGTGCAGCTCGCCGACCACTACCAGCAGAACACC
CCCATCGGCGACGGCCCCGTGCTGCTGCCCGACAACCACTACCT
GAGCTACCAGTCCGCCCTGAGCAAAGACCCCAACGAGAAGCGC
GATCACATGGTCCTGCTGGAGTTCGTGACCGCCGCCGGGATCAC
TCTCGGCATGGACGAGCTGTACAAG*GAATTC*

RhoA wild type (XhoI)

ATGGCTGCCATCCGGAAGAAACTGGTGATTGTTGGTGATGGAG
CCTGTGGAAAGACATGCTTGCTCATAGTCTTCAGCAAGGACCAG
TTCCCAGAGGTGTATGTGCCCACAGTGTTTGAGAACTATGTGG
CAGATATCGAGGTGGATGGAAAGCAGGTAGAGTTGGCTTTGTG
GGACACAGCTGGGCAGGAAGATTATGATCGCCTGAGGCCCCTC
TCCTACCCAGATACCGATGTTATACTGATGTGTTTTTCCATCGAC
AGCCCTGATAGTTTAGAAAACATCCCAGAAAAGTGGACCCCAG
AAGTCAAGCATTTCTGTCCCAACGTGCCCATCATCCTGGTTGGG
AATAAGAAGGATCTTCGGAATGATGAGCACACAAGGCGGGAGC
TAGCCAAGATGAAGCAGGAGCCGGTGAAACCTGAAGAAGGCAG
AGATATGGCAAACAGGATTGGCGCTTTTGGGTACATGGAGTGTT
CAGCAAAGACCAAAGATGGAGTGAGAGAGGTTTTTGAAATGGC
TACGAGAGCTGCTCTGCAAGCTAGACGTGGGAAGAAAAAATCT
GGGTGCCTTGTCTTGTGAAACTAA*CTCGAG*

VIII. Appendix II

A. Media Formulation for Ham's F-12K Phenol Red-Free (Kaighn, 1973; Robey and Termine, 1985)

Volume: 500 mL; without glutamine, pH 7.4 to 7.5

Formulation:			
Inorganic salts	mg/liter	Other compounds	mg/liter
NaCl	7530.00	Glucose	1260.00
KCl	285	Linoleic acid	0
$MgCl_2 \bullet 6H_2O$	106	Hypoxanthine•Na	4
$MgSO_4 \bullet 7H_2O$	393	Phenol red	0
$CaCl_2$	135	Putresine•HCl	0.3

$Na_2HPO_4 \bullet 7H_2O$	218	Sodium pyruvate	220
KH_2PO_4	59	Thymidine	0.7
$NaHCO_3$	2500.00		
$FeSO_4 \bullet 7H_2O$	0.8		
$CuSO_4 \bullet 5H_2O$	2 μg		
$ZnSO_4 \bullet 7H_2O$	0.14		
Amino acids	**mg/liter**	**Vitamins**	**mg/liter**
L-Alanine	17.8	L-Ascorbic acid	0
L-Arginine•HCl	421.3	Biotin	0.07
L-Asparagine•H_2O	30	D-Calcium Pantothenate	0.48
L-Aspartic acid	26.6	Choline chloride	13.96
L-Cysteine•HCl•H_2O	70.04	Cyanocobalamin	1.36
L-Cystine	0	Folic acid	1.32
L-Glutamic acid	29.4	Inositol	18
Glycine	15	Nicotinamide	0.04
L-Histidine•HCl•H_2O	41.9	Pyridoxine•HCl	0.06
L-Isoleucine	7.9	Riboflavin	0.04
L-Leucine	26.2	Thiamine•HCl	0.21
L-Lysine•HCl	73.1	DL-Thioctic acid	0.21
L-Methionine	8.9		
L-Phenylalanine	9.9		
L-Proline	69.1		
L-Serine	21		
L-Threonine	23.8		
L-Tryptophan	4.1		
L-Tyrosine	10.9		
L-Valine	23.4		

References

Adams, S. R., Harootunian, A. T., Buechler, Y. J., Taylor, S. S., and Tsien, R. Y. (1991). Fluorescence ratio imaging of cyclic AMP in single cells. *Nature* **349,** 694–697.

Baird, G. S., Zacharias, D. A., and Tsien, R. Y. (1999). Circular permutation and receptor insertion within green fluorescent proteins. *Proc. Natl. Acad. Sci. USA* **96,** 11241–11246.

Bokoch, G. M., Bohl, B. P., and Chuang, T. H. (1994). Guanine nucleotide exchange regulates membrane translocation of Rac/Rho GTP-binding proteins. *J. Biol. Chem.* **269,** 31674–31679.

Chalfie, M., Tu, Y., Euskirchen, G., Ward, W. W., and Prasher, D. C. (1994). Green fluorescent protein as a marker for gene expression. *Science* **263,** 802–805.

Chamberlain, C. E., Kraynov, V., and Hahn, K. M. (2000). Imaging spatiotemporal dynamics of Rac activation *in vivo* with FLAIR. *Meth. Enzymol.* **325,** 389–400.

Chuang, T.-H., Xu, X., Knaus, U. G., Hart, M. J., and Bokoch, G. M. (1993). GDP dissociation inhibitor (GDI) prevents intrinsic and GTPase activating protein (GAP)-stimulated GTP hydrolysis by the Rac1 and Rac2 GTP-binding proteins. *J. Biol. Chem.* **268,** 775–778.

Del Pozo, M. A., Kiosses, W. B., Alderson, N. B., Meller, N., Hahn, K. M., and Schwartz, M. A. (2002). Integrins regulate GTP-Rac localized effector interactions through dissociation of Rho-GDI. *Nat. Cell Biol.* **4,** 232–239.

DerMardirossian, C., and Bokoch, G. M. (2005). GDIs: Central regulatory molecules in Rho GTPase activation. *Trends Cell Biol.* **15,** 356–363.

dos Remedios, C. G., and Moens, P. D. (1995). Fluorescence resonance energy transfer spectroscopy is a reliable "ruler" for measuring structural changes in proteins. Dispelling the problem of the unknown orientation factor. *J. Struct. Biol.* **115,** 175–185.

Gordon, G. W., Berry, G., Liang, X. H., Levine, B., and Herman, B. (1998). Quantitative fluorescence resonance energy transfer measurements using fluorescence microscopy. *Biophys. J.* **74,** 2702–2713.

Hahn, K., DeBiasio, R., and Taylor, D. L. (1992). Patterns of elevated free calcium and calmodulin activation in living cells. *Nature* **359,** 736–738.

Haj, F. G., Verveer, P. J., Squire, A., Neel, B. G., and Bastiaens, P. I. (2002). Imaging sites of receptor dephosphorylation by PTP1B on the surface of the endoplasmic reticulum. *Science* **295,** 1708–1711.

Heikal, A. A., Hess, S. T., Baird, G. S., Tsien, R. Y., and Webb, W. W. (2000). Molecular spectroscopy and dynamics of intrinsically fluorescent proteins: Coral red (dsRed) and yellow (Citrine). *Proc. Natl. Acad. Sci. USA* **97,** 11996–12001.

Heim, R., and Tsien, R. Y. (1996). Engineering green fluorescent protein for improved brightness, longer wavelengths and fluorescence resonance energy transfer. *Curr. Biol.* **6,** 178–182.

Hodgson, L., Nalbant, P., Shen, F., and Hahn, K. (2006). Imaging and photobleach correction of Mero-CBD, sensor of endogenous Cdc42 activation. *Meth. Enzymol.* **406,** 140–156.

Kaighn, M. E. (1973). "Tissue Culture Methods and Applications," pp. 54–56. Academic Press, New York.

Kenworthy, A. K. (2001). Imaging protein–protein interactions using fluorescence resonance energy transfer microscopy. *Methods* **24,** 289–296.

Kraynov, V. S., Chamberlain, C., Bokoch, G. M., Schwartz, M. A., Slabaugh, S., and Hahn, K. M. (2000). Localized Rac activation dynamics visualized in living cells. *Science* **290,** 333–337.

Lakowicz, J. R. (1999). "Principles of Fluorescence Spectroscopy," pp. 368–377. Kluwer Academic/Plenum, New York.

Llopis, J., Westin, S., Ricote, M., Wang, Z., Cho, C. Y., Kurokawa, R., Mullen, T. M., Rose, D. W., Rosenfeld, M. G., Tsien, R. Y., and Glass, C. K. (2000). Ligand-dependent interactions of coactivators steroid receptor coactivator-1 and peroxisome proliferator-activated receptor binding protein with nuclear hormone receptors can be imaged in live cells and are required for transcription. *Proc. Natl. Acad. Sci. USA* **97,** 4363–4368.

Michaelson, D., Silletti, J., Murphy, G., D'Eustachio, P., Rush, M., and Philips, M. R. (2001). Differential localization of Rho GTPases in live cells: Regulation by hypervariable regions and RhoGDI binding. *J. Cell Biol.* **152,** 111–126.

Miyawaki, A., Llopis, J., Heim, R., McCaffery, J. M., Adams, J. A., Ikura, M., and Tsien, R. Y. (1997). Fluorescent indicators for Ca^{2+} based on green fluorescent proteins and calmodulin [see comments]. *Nature* **388,** 882–887.

Miyawaki, A., and Tsien, R. Y. (2000). Monitoring protein conformations and interactions by fluorescence resonance energy transfer between mutants of green fluorescent protein. *Meth. Enzymol.* **327,** 472–500.

Nagai, T., Yamada, S., Tominaga, T., Ichikawa, M., and Miyawaki, A. (2004). Expanded dynamic range of fluorescent indicators for $Ca(^{2+})$ by circularly permuted yellow fluorescent proteins. *Proc. Natl. Acad. Sci. USA* **101,** 10554–10559.

Nalbant, P., Hodgson, L., Kraynov, V., Toutchkine, A., and Hahn, K. M. (2004). Activation of endogenous Cdc42 visualized in living cells. *Science* **305,** 1615–1619.

Nguyen, A. W., and Daugherty, P. S. (2005). Evolutionary optimization of fluorescent proteins for intracellular FRET. *Nat. Biotechnol.* **23,** 355–360.

Periasamy, A. (2001). Fluorescence resonance energy transfer microscopy: A mini review. *J. Biomed. Opt.* **6,** 287–291.

Periasamy, A., and Day, R. N. (1999). Visualizing protein interactions in living cells using digitized GFP imaging and FRET microscopy. *Methods Cell Biol.* **58,** 293–314.

Pertz, O., Hodgson, L., Klemke, R. L., and Hahn, K. M. (2006). Spatiotemporal dynamics of RhoA activity in migrating cells. *Nature* **440,** 1069–1072.

Robey, P. G., and Termine, J. D. (1985). Human bone cells *in vitro*. *Calcif. Tissue Int.* **37,** 453–460.

Taylor, D. L., and Wang, Y. L. (1980). Fluorescently labeled molecules as probes of the structure and function of living cells. *Nature* **284,** 405–410.

Ting, A. Y., Kain, K. H., Klemke, R. L., and Tsien, R. Y. (2001). Genetically encoded fluorescent reporters of protein tyrosine kinase activities in living cells. *Proc. Natl. Acad. Sci. USA* **98,** 15003–15008.

Tzima, E., Kiosses, W. B., del Pozo, M. A., and Schwartz, M. A. (2003). Localized cdc42 activation, detected using a novel assay, mediates microtubule organizing center positioning in endothelial cells in response to fluid shear stress. *J. Biol. Chem.* **278,** 31020–31023.

Whitlow, M., Bell, B. A., Feng, S. L., Filpula, D., Hardman, K. D., Hubert, S. L., Rollence, M. L., Wood, J. F., Schott, M. E., Milenic, D. E., Takashi, Y., and Schlom, J. (1993). An improved linker for single-chain Fv with reduced aggregation and enhanced proteolytic stability. *Protein Eng.* **6,** 989–995.

Xia, Z., and Liu, Y. (2001). Reliable and global measurement of fluorescence resonance energy transfer using fluorescence microscopes. *Biophys. J.* **81,** 2395–2402.